

DEVELOPMENTAL ANALYSIS OF *TEOSINTE GLUME ARCHITECTURE1*: A KEY LOCUS IN THE EVOLUTION OF MAIZE (POACEAE)¹

JANE E. DORWEILER² AND JOHN DOEBLEY³

Department of Plant Biology, University of Minnesota, St. Paul, Minnesota 55108

A key event in the evolution of maize from teosinte was a reduction in the cupulate fruitcase and softening of the glumes, which increased the accessibility of kernels for harvest. The *teosinte glume architecture1* (*tga1*) locus largely controls this difference between maize and teosinte, and thus may have played a pivotal role in maize evolution. The teosinte allele (*tga1+teosinte*) lengthens inflorescence internodes, shortens rachillae, and makes glumes longer, thicker, and harder. Developmental characterization of morphometric traits reveals that differences among genotypes are apparent early in female inflorescence development. Increased hardening in glumes homozygous for *tga1+teosinte* is correlated with a thicker abaxial mesoderm of lignified cells. Silica deposition in the abaxial epidermal cells of the glumes is also affected. In the maize background, glumes homozygous for *tga1+teosinte* deposit silica in both the short and long cells of the glume epidermis, whereas glumes homozygous for the maize allele (*Tga1+Maize*) concentrate silica only in the short cells. Silica deposition also appears to be affected by genetic background. The effects of *tga1* appear largely to explain the differences in glume induration between maize and teosinte. The diverse pleiotropic effects of *tga1* suggest that it is regulatory in nature.

Key words: domestication; genetics; inflorescence; maize; Poaceae; quantitative trait locus; *Zea mays*.

Development represents the key connection between genetic variation and phenotypic diversity upon which natural selection operates. The past decade has witnessed exponential growth in interest in the evolution of development, with a particular emphasis on understanding the evolution of developmental mechanisms that underlie pattern formation in diverse organisms (Raff, 1992; Carroll, 1994; Coen and Nugent, 1994; Patel, 1994; Curtis, Apfeld and Lehmann, 1995; Holland and Garcia-Fernandez, 1996). Another focus of interest has been on changes of the genetic architecture that underlie morphological evolution (Bachmann, 1983; Gottlieb, 1984; Orr and Coyne, 1992; Doebley, 1993). This latter topic has been of particular interest among plant evolutionists since in plants one often finds radical morphological differences between cross-compatible species or different varieties of a single species. This feature of plant systems makes them ideal for the investigation of the genetic basis of the morphological differences among species.

Maize (*Zea mays* L. ssp. *mays*) offers a powerful system for studying the genetic and developmental basis of morphological evolution. The maize ear (or female inflorescence) possesses a multitude of striking differences from the ear of its wild progenitor, teosinte (*Zea mays* ssp. *parviglumis* Iltis and Doebley). One of the key dif-

ferences between the maize and teosinte ears is the architecture of the outer glume and its associated rachis segment (cupule). The outer glume is a bract, which subtends each kernel on the ear. In maize, the outer glume is small and obscure, being visible only once the kernels have been removed from the cob (Fig. 1). The glume is more prominent on a teosinte female inflorescence, growing around the kernel and together with the rachis, completely encasing the kernel (Fig. 1). Thus, the glume and rachis of teosinte make the teosinte kernel quite inaccessible and difficult to harvest. Maize is also characterized by softer, more reflexed glumes relative to the hard ("stony"), erect glumes of teosinte. Associated with differences in the glume are differences in the rachilla (or pedicel) on which the kernel is borne. The rachilla of maize is elongated such that the kernel projects from the ear, whereas the rachilla of teosinte fails to elongate so that the kernel fits tightly into the associated fruitcase (Galinat, 1957).

Previous work identified a quantitative trait locus (QTL) on maize chromosome 4 that largely controls the differences in glume hardness between maize and teosinte (Doebley and Stec, 1991, 1993). Subsequently, it was shown that this QTL corresponds to a single major Mendelian locus (*teosinte glume architecture1*, *tga1*), and that this locus has a major effect on the architecture of several aspects of cupulate fruitcase morphology (Dorweiler et al., 1993). In this study, we document the macroscopic and microscopic effects of *tga1* on ear development. We show that the teosinte allele (*tga1+teosinte*) increases the length, thickness, and curvature of the glume, length of the inflorescence internodes, the cellular deposition of crystalline silica, and the pattern of lignification of glume cells. Maize ears homozygous for *tga1+teosinte* produce prominent glumes, which successfully envelop the basal portion of the kernel. The effects of *tga1+teosinte* in maize background are those that would contribute posi-

¹ Manuscript received 8 November 1996; revision accepted 26 February 1997.

The authors thank Adrian Stec for valuable technical assistance; and Elizabeth Kellogg, Neil Olszewski, Ruth Shaw, Marshall Sundberg, and Shawn White for helpful comments on the manuscript; and Dr. Anne Sylvester for suggesting the analysis of silica deposition using X-ray microanalysis and teaching one of us (JED) this and several other microscopy techniques. This research was supported by NSF grants BSR-9107175, MCB-9513573 and partial support from NSF Grants BIR-9214615 and BIR-9313813.

² Current address: Department of Plant Sciences, University of Arizona, Tucson AZ 85721.

³ Author for correspondence.

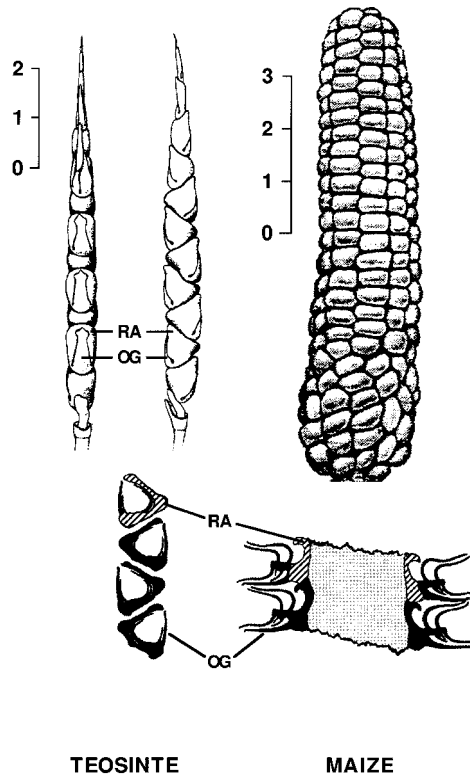


Fig. 1. Sketches of whole (above) and longitudinal sections (below) of teosinte (left) and maize (right) female inflorescences showing the cupulate fruitcase architecture. Kernels are not visible (encased) in the teosinte inflorescence, and they are not drawn in the longitudinal sections. The hatched area represents the rachis internode. The outer glume and rachis internode are not visible on the complete maize ear. Adapted from Galinat (1969) and Iltis (1983).

Figure Abbreviations: I, immature ears; l, long cells; M, mature stage; OG, outer glume; P, pollination stage; RA, rachis or rachis internode; s, short (silica) cells.

tively to the fitness of a wild grass, whereas the loss of these same features contributes positively to the value of maize as a crop. Thus, the evolution of the *Tgal + Maize* allele represents a critical step in maize evolution. We argue that the novel phenotype and diverse pleiotropic effects of *tgal* suggest that it is likely to be regulatory in nature.

MATERIALS AND METHODS

Plant material—The effects of *tgal* on ear development were analyzed by comparing the effects of the maize and teosinte alleles in the uniform genetic background of maize inbred line W22. To do this, we employed standard W22 possessing the maize allele (*Tgal + Maize*) at *tgal*, and a modified W22, called W22-TGA, which possesses the teosinte allele (*tgal + teosinte*) at *tgal* (Dorweiler et al., 1993). To observe the effects of *Tgal + Maize/tgal + teosinte* heterozygotes, F_1 hybrids of W22 and W22-TGA were also analyzed. The source of the teosinte allele in W22-TGA was *Z. mays* ssp. *mexicana* Wilkes 48703. Developmental analyses on both lines and their hybrid were conducted on plants grown in the research fields of the University of Minnesota during the summers of 1993 and 1994.

To observe the effects of *tgal* in the teosinte background, some analyses were also done on teosinte plants homozygous for either the teosinte allele (*tgal + teosinte*) or the maize allele (*Tgal + Maize*). We used

backcross breeding with molecular-marker-assisted selection to transfer a region of the maize chromosome arm *4S* encompassing the *tgal* locus into teosinte background (Dorweiler et al., 1993). The starting material for this backcross breeding program was an F_2 population based on a cross of Reventador maize (Nay 15) and teosinte (*Z. mays* ssp. *parviglumis* Iltis and Cochrane 81) that was previously analyzed by Doebley and Stec (1993). Individual F_2 plants were selfed, providing a series of F_3 families. A single F_3 plant homozygous for the maize allele at all marker loci in the target region of chromosome arm *4S*, but which carried teosinte alleles at most marker loci outside the target region, was selected. This selected F_3 plant was backcrossed to teosinte for three generations before selfing to produce a BC_3F_2 population. Molecular markers were employed each generation of the backcross breeding program to insure that we were retaining the maize allele in the target region as well as eliminating maize alleles outside the target region. Marker loci outside the target region were specifically chosen to eliminate regions of the genome that possess QTL contributing to the morphological differences between maize and teosinte. In the BC_3F_2 population, teosinte plants homozygous for the maize (*Tgal + Maize*) allele at *tgal* were identified and selfed.

Developmental measurements—In order to assess the effects of the maize and teosinte alleles at *tgal* on the rate of glume and ear growth, the size of these structures was measured at several developmental stages. These measurements were done on fresh material, with the exception of mature ears, which were allowed to fully dehydrate, and a few of the smallest ears, which were fixed in FAA (4% formaldehyde, 5% glacial acetic acid, and 50% ethanol) or 2.5% glutaraldehyde (using a 0.1 mol/L sodium phosphate buffer, pH 6.8) for later measurement. The youngest ear shoots were removed from the 6th to 7th leaf sheath (counting from the base of the plant) just before they emerged from the sheath. After emergence from the leaf sheath, sampling was restricted to the first and second ear shoots, which were typically but not always located in the axils of the 6th–7th leaves. All measurements, with the exception of structures greater than two centimeters in length, were made on a dissecting microscope using an optical micrometer.

In order to determine when the effects of *tgal* are first manifest, we defined specific stages of ear/spikelet development at which to compare the size of various structures. All measurements were made on the 4th–6th spikelet from the base of the ear. These stages are immature (I0–I3), postpollination (P0–P3), and mature (M). The earliest stage examined (I0) is equivalent to stages I–K of Cheng, Greyson, and Walden (1983) with spikelet maturation ranging from the onset of stylar ridge formation surrounding the gynoecial apex (I) to the time of stamen abortion in the upper floret (K). Stage I0 includes spikelets whose stigma or silk were <1 mm long. Stages I1–I3 were defined as to the degree of silk elongation until the time of silk emergence. Stage I1 includes spikelets with silks >0.1 cm, but <5 cm. Stage I2 includes spikelets with silks ≥ 5 cm but <10, and stage I3 includes spikelets with silks 10–15 cm long. Upon silk emergence (silks ~ 15 cm or longer), ears are mature enough for pollination and were defined as stage P0. After pollination, the ears are referred to as stage Px with x representing the number of weeks postpollination. We analyzed ears of stages P1, P2, and P3, which had been pollinated 1, 2, and 3 wk prior to their analysis, respectively. Stage M refers to mature ears, which were pollinated minimally 5 wk prior to harvest and then allowed to fully dehydrate before analysis.

Measurements made included internode length, glume thickness, glume length, and rachilla length. Internode length was measured near the base of the ear by measuring the total length of 5–10 internodes (cupules) and then dividing by that number to get the average internode length. Glume thickness was measured near the base of the glume after slicing through the glume laterally. On a mature glume, the position measured was ~ 1.5 –2 mm above the point where the adaxial surface of the glume and the lemma joins the rachilla. Glume length was measured centrally from the base of the glume to the apical margin. One-

way Analysis of Variance (ANOVA) was used to test for statistically significant differences among genotypes.

Rachilla length was measured on mature ears only. The rachilla is the pedicel on which the kernel is borne. A segment of the rachilla was measured from the point of inner glume attachment to the point of kernel abscission, as these were the two most clearly defined positions along the rachilla in this background. This measurement was made after the kernels had been removed and the ear was then cut longitudinally using a fine-toothed band saw.

Scanning electron microscopy—Scanning electron microscopy (SEM) was employed to study and document the three-dimensional shape of developing glumes and to examine the surface detail of the abaxial epidermis of developing glumes. Specimens for SEM were prepared in one of two ways. (1) The whole spikelet specimens were prepared using a dental impression medium as a mold for a resin replica of the sample (Williams and Sylvester, 1994). (2) Specimens used for higher magnification were fixed in 2.5% glutaraldehyde solution using a 0.1 mol/L sodium phosphate buffer (pH 6.8), rinsed twice in buffer alone, dehydrated in an ethanol series, and dried using a Tousimis Autosam-dri-814 critical point dryer (Williams and Sylvester, 1994). Samples were then coated with gold-palladium using a Denton DV-502 vacuum evaporator and examined using a Hitachi S-450 scanning electron microscope at an accelerating voltage of 5–10 kV.

Fluorescence microscopy—Fluorescence microscopy was used to detect early signs of glume lignification due to changes in the wavelength of emitted light from ultraviolet (UV) excited tissue (Harris and Hartley, 1976). These changes in fluorescence were confirmed to be due to lignification by testing with 0.1 mol/L ammonium hydroxide as suggested by Harris and Hartley (1976). The earliest precursors of lignin fluoresce a very light shade of violet. As lignification progresses, the sample fluoresces in a deeper shade of violet. This technique allows the visualization of precursors to lignin in glume crosssections. Microscopy was done on either fresh material, or material fixed in FAA and later rehydrated by successive washes in 50 and 25% ethanol and then distilled H₂O. All samples were chilled to 4°C for maximum turgidity before freehand sectioning (Sylvester and Ruzin, 1994). Freehand sections were then examined under UV irradiation at 365 nm on a Zeiss Axioskop microscope fitted with a Zeiss MC80 camera. Photographs were taken using Kodak 160T Ektachrome film.

X-ray microanalysis—X-ray microanalysis was used to examine the pattern and extent of silica deposition in the abaxial epidermal cells of the glume and rachid. X-ray microanalysis was done on frozen-hydrated specimens prepared as described by Zeyen, Ahlstrand, and Carver (1993) using a Philips 500X SEM equipped with an EDAX International System 711F energy-dispersive x-ray microanalysis unit and a Philips cold stage. All quantitative measurements were standardized as described by Zeyen, Ahlstrand, and Carver (1993) with the exception that the SEM beam current was adjusted to a consistent count rate on the gold of the cold stage rather than on bare aluminum at the stub margin. Silica counts were averaged over three intervals of 40 s each on the individual glumes examined. Silica dot maps were generated for qualitative results, and thus the time interval was varied to give an informative picture consisting of a minimum of ~38K counts.

RESULTS

Morphometric effects of *tga1*—As compared to the mature *Tgal+Maize* homozygote, the ears of mature *tga1+teosinte* homozygotes have longer internodes, thicker glumes, longer glumes, and shorter rachillae (Figs. 2–4, Table 1). *tga1* has an additive effect on each of these quantitative traits. Measurements of the heterozygote generally fall between the two homozygous class-

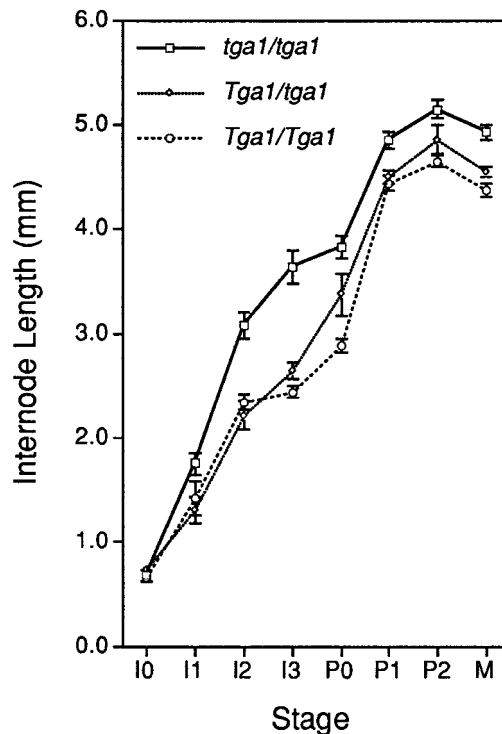


Fig. 2. Internode length among *tga1* genotypes vs. developmental stage. The difference in inflorescence internode length is apparent from relatively early stages, with the *tga1+teosinte* homozygotes having the longest internodes. Stages are (I) immature, (P) postpollination, and (M) mature, but are described thoroughly in Materials and Methods. Error bars depict SE of the mean.

es, though they more closely resemble values in the maize allele homozygote, suggesting partial dominance of the maize allele (Figs. 2–4, Table 1). The magnitude of the difference between the *tga1+teosinte* homozygote and the *Tgal+Maize* homozygote at maturity ranges from roughly a 10% increase in internode length to an approximate doubling of glume thickness and length (Figs. 2–4, Table 1). With respect to mature rachilla length, *Tgal+Maize* homozygotes have the longest rachillae, and *tga1+teosinte* homozygotes have much shorter rachillae (Table 1).

Time of *tga1* expression—In order to determine when differences among *tga1* genotypes are first manifest, internode length, glume thickness, and glume length were measured on maize ears of each genotype at specific developmental stages. The first visible effect of *tga1* is on internode length at stage I1, by which time the *tga1+teosinte* homozygote has significantly longer internodes than the other genotypes (Fig. 2). Differences in glume length among genotypes are also apparent ($P = 0.04$) by stage I1, though more convincingly so at stage I2 ($P = 0.0001$) (Fig. 3). Pairwise comparisons of genotypes reveal that glumes and inflorescence internodes of *tga1+teosinte* homozygotes are significantly longer than those of heterozygotes and *Tgal+Maize* homozygotes by stage I2, whereas heterozygotes and *Tgal+Maize* homozygotes are significantly different from one another at stage I3 for glumes and stage P0 for

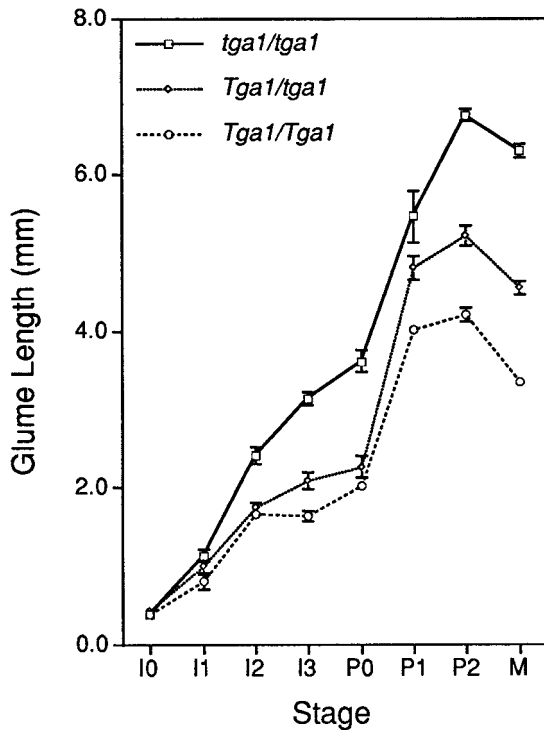


Fig. 3. Glume length among *tga1* genotypes vs. developmental stage. The difference in the length of female inflorescence glumes between *tga1+teosinte* homozygotes and the other two genotypes becomes apparent prior to pollination. The difference between *Tga1+Maize* homozygotes and heterozygotes becomes consistent by the time ears are mature enough for pollination. Stages are (I) immature, (P) postpollination, and (M) mature, but are described thoroughly in Materials and Methods. Error bars depict SE of the mean.

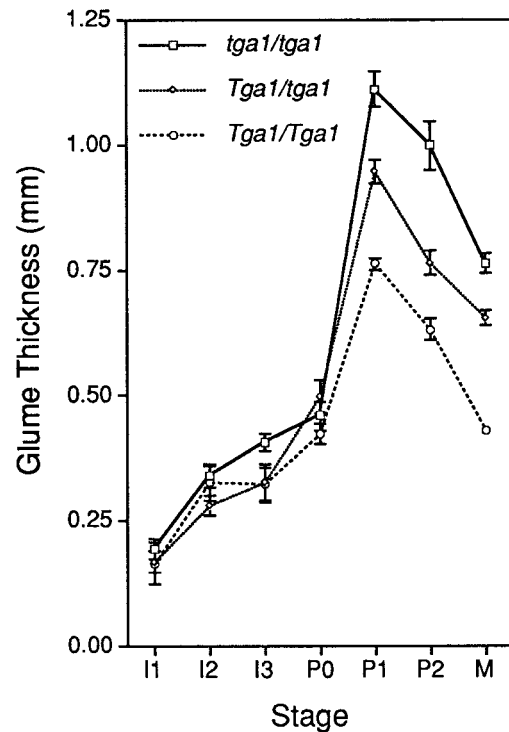


Fig. 4. Glume thickness among *tga1* genotypes vs. developmental stage. The differences among genotypes in thickness of female inflorescence glumes are only apparent after pollination, and persist as dehydrating glumes shrink in thickness. *Tga1+teosinte* homozygotes have the thickest glumes. Stages are (I) immature, (P) postpollination, and (M) mature, but are described thoroughly in Materials and Methods. Error bars depict SE of the mean.

internodes (Figs. 2–3). This delayed differentiation between heterozygotes and *Tga1+Maize* homozygotes reflects the partially dominant nature of the *Tga1+Maize* allele. Significant differences in glume thickness are only apparent in postpollination ears. Prior to that time, differences in the expected direction exist but fall below the level of statistical significance, perhaps in part due to difficulty in measuring this trait precisely in immature ears (Fig. 4).

Scanning electron microscopy—Scanning electron micrographs show the differences in glume shape between the *Tga1+Maize* homozygote, *tga1+teosinte* homozygote, and heterozygote. *Tga1+Maize* homozygote glumes are relatively angular, frequently planar at maturity, and short, being shortest at midglume due to a groove surrounded by numerous trichomes (Fig. 5). Heterozygotes are more rounded, but still possess a mid-glume groove (Fig. 6). *tga1+teosinte* homozygous glumes are longer and more rounded, more fully surrounding the developing kernel, possessing only a slight groove with a few trichomes at the upper margin (Fig. 7). An interesting feature of the *tga1+teosinte* homozygotes is that as the underlying kernel develops, it often causes tearing of the upper margin of the glume to accommodate the kernel's increasing size, whereas in maize homozygotes, since the glume is shorter and straighter as

well as more pliable, it can accommodate the developing kernel without tearing.

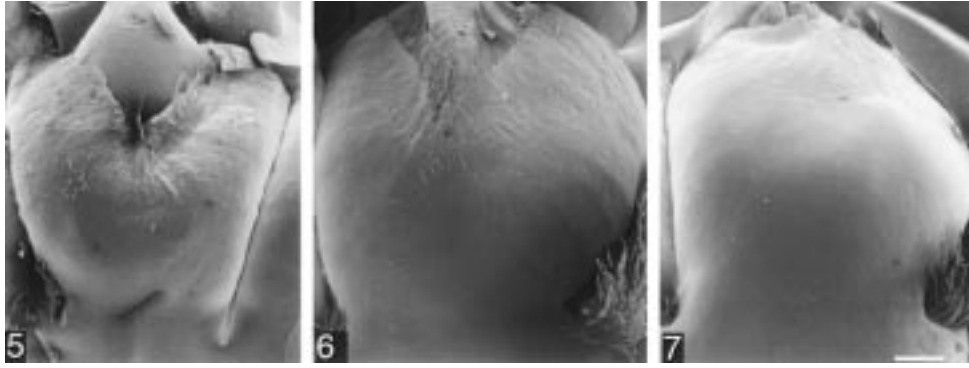
A closer look at the abaxial epidermal surface of the glume reveals additional effects of *tga1*. Glumes of all three genotypes have epidermal characteristic of grass leaves, composed of long and short cells, but differ in the relative proportions of each cell type (Figs. 8–10). *Tga1+Maize* homozygotes have numerous short (silica) cells, whereas *tga1+teosinte* homozygotes have very few short cells (Figs. 8, 10). Heterozygotes are most like *Tga1+Maize* homozygotes, having prevalent silica cells (Figs. 8, 9). Also apparent from comparison of the genotypes is the relatively rough texture of *Tga1+Maize* homozygotes and heterozygotes compared to the much smoother surface of *tga1+teosinte* homozygotes (Figs. 8–10). This difference is visible when examining glumes with the naked eye in that glumes of *tga1+teosinte* ho-

TABLE 1. Mean rachilla length for the three genotypic classes at *tga1*.

Genotype ^a	Rachilla length (mm) ^b	SD
<i>Tga1 + Maize/Tga1 + Maize</i>	1.964	0.319
<i>Tga1 + Maize/tga1 + teosinte</i>	1.828	0.253
<i>tga1 + teosinte/tga1 + teosinte</i> *	1.314	0.283

^a Analysis of variance among genotypes significant at $P = 0.0001$; * signifies pairwise comparisons with other two genotypes significant at $>95\%$.

^b $N = 19$ in all cases.



Figs. 5–7. Representative shape differences between the three genotypes at *tgal*. **5.** Glume of a *Tgal+Maize* homozygote. Note the prominent apical groove, and the angular curves near the sides of the glume (i.e., it would surround the developing spikelet on three sides). **6.** Glume of a heterozygote. Note that the apical groove is still apparent, and that the glume is approaching a rounder shape such that it surrounds three sides and part of the apical portion of the developing spikelet. **7.** Glume of a *tgal+teosinte* homozygote. The apical groove is considerably less prominent,

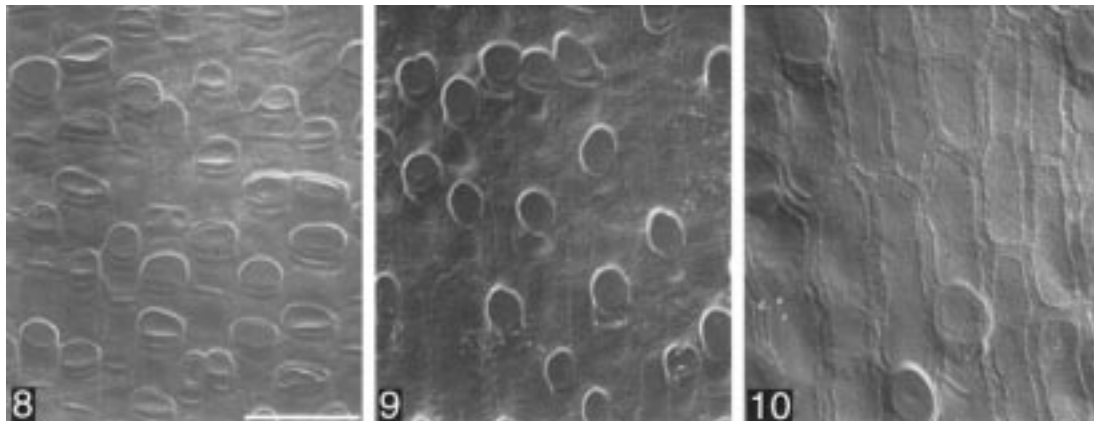
mozygotes are shiny, whereas those of *Tgal+Maize* homozygotes and heterozygotes have a relatively dull appearance.

Fluorescence microscopy—Fluorescence microscopy was used to detect early signs of lignification due to changes in the wavelength of emitted light from UV excited tissue. Glume cross sections from developing ears revealed no signs of lignification-related fluorescence at or prior to the pollination stage (P0). By 1 wk postpollination (P1), early signs of lignification are apparent in all three genotypes as a light violet fluorescence of the abaxial mesoderm, and there are no apparent differences among genotypes (Figs. 11–13). By 2 wk postpollination (P2), lignification in the *Tgal+Maize* homozygotes appears nearly complete, whereas the *tgal+teosinte* homozygote fluorescence is consistent with still having only the precursors of lignin (Figs. 14–16). Once glumes have become completely lignified, they are often characterized by thicker walls, a narrow lumen, and the contrast of “halos” of white fluorescence adjacent to the lumen of each cell surrounded by a deep-violet fluorescence from the intercellular matrix. Even at maturity, glumes of the *tgal+teosinte* homozygotes often fail to become as com-

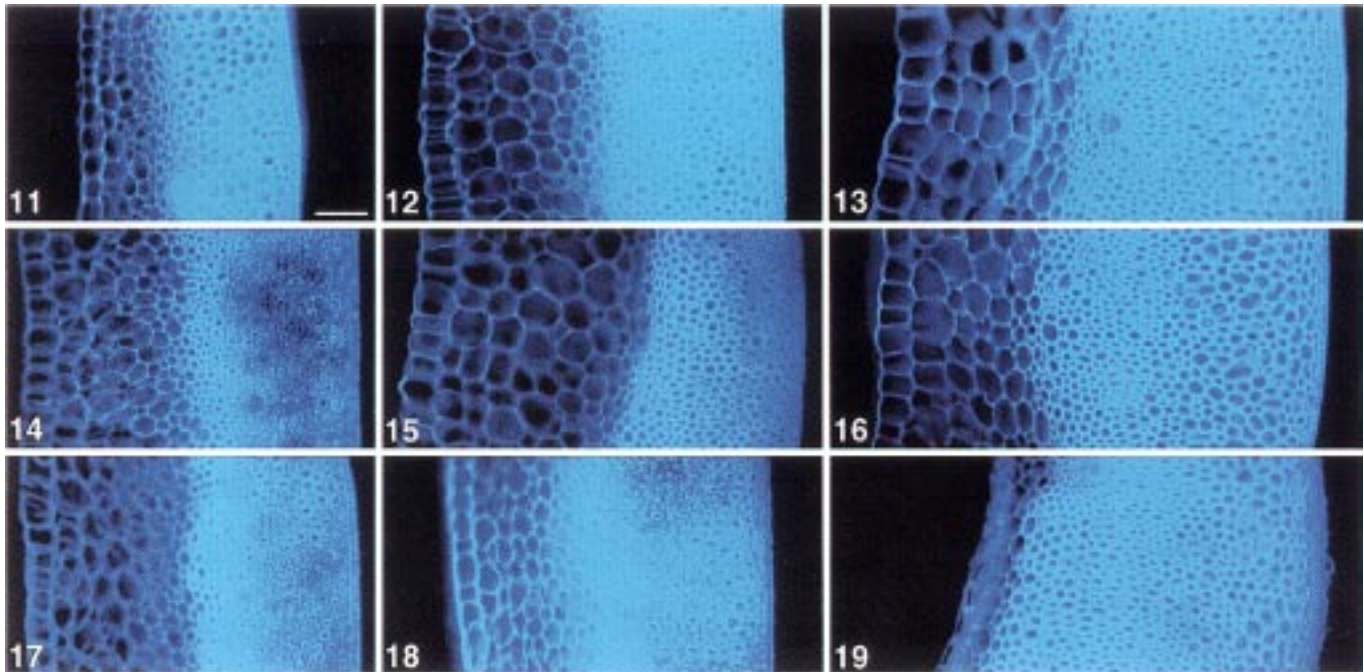
pletely lignified as the *Tgal+Maize* homozygotes to the extent that they fail to show a consistent “halo” effect with strongly contrasting lumen vs. intercellular matrix (Figs. 17–19). This was unexpected since *tgal+teosinte* homozygous glumes are in fact more rigid.

Perhaps the most interesting observation from the cross sections of glumes of each genotype is the fact that, though each glume is divided into an abaxial mesoderm composed of small cells, which become lignified, and an adaxial mesoderm composed of larger parenchyma cells, the abaxial mesoderm is considerably thicker in *tgal+teosinte* homozygotes. The thicker abaxial mesoderm in *tgal+teosinte* homozygotes is attributed to a larger number of cells in that layer than in the *Tgal+Maize* homozygotes or heterozygotes (Table 2). This suggests that differences in glume hardness are due to a higher number of lignified cells rather than increased lignification of those cells. At maturity the adaxial mesoderm of parenchyma cells dehydrates and collapses, whereas the abaxial mesoderm remains intact due to the more rigid, lignified cell walls (cf. Fig. 19).

Silica deposition in epidermal cells—X-ray microanalysis revealed silica deposition in the glumes of both



Figs. 8–10. Abaxial epidermis of pistillate glumes of each genotype at 3 wk postpollination. **8.** *Tgal+Maize/Tgal+Maize*. **9.** *Tgal+Maize/tgal+teosinte*. **10.** *tgal+teosinte/tgal+teosinte*. Note the relative abundance of short cells, and the relative visibility and shape of cell walls separating intervening long cells. Bar = 50 μ m for all three images.



Figs. 11–19. Lignification in postpollination maize glumes. Glume sections are shown for 1 wk (11–13), 2 wk (14–16), and 3 wk (17–19) postpollination (Stages P1, P2, and P3). Genotypes shown are *Tgal+Maize/Tgal+Maize* (Figs. 11, 14, 17), *Tgal+Maize/tgal+teosinte* (Figs. 12, 15, 18) and *tgal+teosinte/tgal+teosinte* (Figs. 13, 16, 19). Glume cross sections are oriented such that the adaxial epidermis is to the left, and the abaxial epidermis to the right. Fluorescence microscopy reveals lignification in the abaxial mesoderm of maize glumes of all three genotypes at *tgal*, and progressive lignification in each postpollination stage. In P3 stage glumes, the *Tgal+Maize* homozygote (Fig. 17) appears nearly fully lignified, whereas the *tgal+teosinte* homozygote (Fig. 19) shows less lignification. Bar = 50 μ m for all nine images.

maize and teosinte. Glumes from maize ears representing the three genotypes at *tgal* in the W22 background were examined. We found that the standard W22 line (*Tgal+Maize/Tgal+Maize*) has high concentrations of silica in the short cells of the glumes, but that the long cells have virtually no deposition of silica. This is evident from a low density of silica dots for long cells that is no greater than background levels as compared to a high density of silica dots for short cells (Figs. 20–21). The heterozygotes have a similar silica distribution to *Tgal+Maize* homozygotes, suggesting dominance of the maize allele (Figs. 22–23). The *tgal+teosinte* homozygotes, though they have high silica deposition in their short cells, have additional silica deposited in the long cells of the glumes, which appears as the dense scattering of silica dots corresponding to the long cells (Figs. 24–25).

Silica deposition was studied in glumes of stages

TABLE 2. Mean number of abaxial mesoderm cells for the three genotypic classes at *tgal*.

Genotype ^a	Cell number ^b	SD
<i>Tgal + Maize/Tgal + Maize</i>	14.25	2.521
<i>Tgal + Maize/tgal + teosinte</i>	16.69	2.359
<i>tgal + teosinte/tgal + teosinte*</i>	25.06	3.859

^a Analysis of variance among genotypes significant at $P = 0.0001$; * signifies pairwise comparisons with other two genotypes significant at $>95\%$.

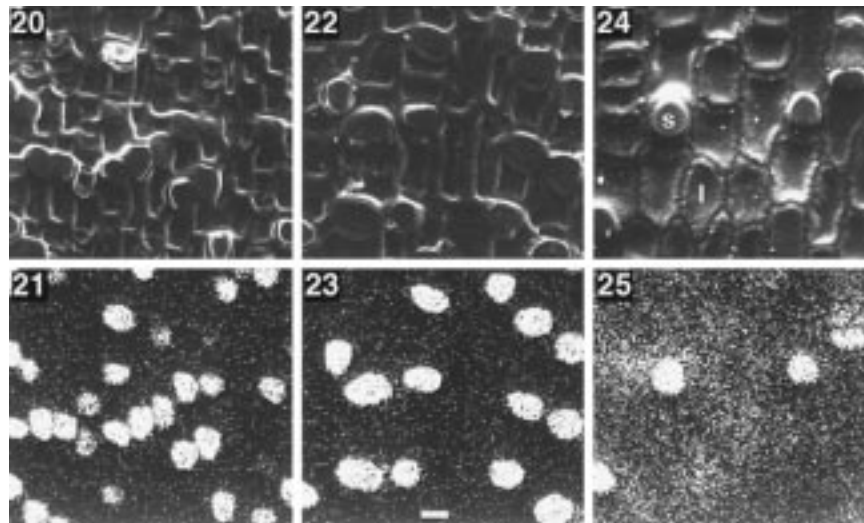
^b $N = 8$ in all cases.

P0–P3 and M. Glumes at the P0 stage showed little or no silica deposition. Glumes of stages P1–P3 showed similar patterns of silica distribution to the mature glumes, and did not reveal any evidence for differential rates of silica deposition in each of the genotypes (data not shown).

The amount of silica in the long and short cells was also quantified using X-ray microanalysis. We found no detectable difference in the amount of silica in the short cells of the three genotypes. However, the amount of silica in the long cells of *tgal+teosinte* homozygotes is nearly 40 times the amount of silica in the long cells of both the maize homozygote and the heterozygote (Table 3).

Tassel glumes from plants homozygous at *tgal* in the W22 background were examined. We found no difference in the silica deposition pattern between standard W22 (*Tgal+Maize/Tgal+Maize*) and W22-TGA (*tgal+teosinte/tgal+teosinte*), with both tassel glumes showing silica deposited in the short cells but absent from the long cells (Figs. 26–29). This result indicates that the *tgal* effect on silica is not present in the tassel glumes and is thus restricted to the ear glumes.

Analysis of teosinte plants homozygous at *tgal* reveals similar effects on silica deposition, though comparison with identical genotypes in the maize background reveals that genetic background also impacts the pattern of silica deposition. In the teosinte background, *Tgal+Maize* homozygotes showed a complex pattern of silica deposition (Figs. 30–31). All short cells are filled with silica as seen in the maize background, but some of the long cells also



Figs. 20–25. Silica distribution in maize glumes. SEM micrographs (Figs. 20, 22, 24) of glumes of the three genotypes at *tga1* and their corresponding silica dot maps (Figs. 21, 23, 25). Genotypes shown are *Tga1+Maize/Tga1+Maize* (Figs. 20, 21), *Tga1+Maize/tga1+teosinte* (Figs. 22, 23), and *tga1+teosinte/tga1+teosinte* (Figs. 24, 25). In each micrograph, silica cells (s) are visible. The corresponding dot maps show a high density of silica X-rays (dots) mapping to these silica cells. The *tga1+teosinte* homozygotes also have a high number of silica X-rays mapping to

have silica deposition. In contrast, we observed a stronger, nearly uniform distribution of silica in *tga1+teosinte* homozygotes in teosinte genetic background (Figs. 32–33). Comparison of identical genotypes in the maize and teosinte backgrounds reveals that the teosinte background alters both *tga1* genotypes toward a more uniform distribution of silica and maize background toward concentration of silica in the short cells (compare Figs. 21, 25, 31, and 33). Thus genetic background also has an effect on silica distribution. In the *tga1+teosinte* homozygote, distinct silica cells are apparent in the maize background, but not in the teosinte background (cf. Figs. 25 and 33). In the *Tga1+Maize* homozygote, distinct silica cells are present in both backgrounds, but while in the maize background long cells are virtually devoid of silica, in the teosinte background about half of the long cells are filled with silica (cf. Figs. 21 and 31).

Cupules or rachis segments from teosinte plants homozygous at *tga1* were also examined. Though short cells are not easily identified on the cupule surface of the *Tga1+Maize* homozygotes, the distribution of silica is very patchy and appears to be concentrated into short cells, whereas the level of silica in the surrounding cells is only slightly above background levels (Figs. 34–35). In contrast, *tga1+teosinte* homozygotes show a uniform distribution of silica as found in the glumes (Figs. 36–37).

TABLE 3. Mean silica counts in long cells for the three genotypic classes at *tga1*.

Genotype	Silica counts	SD
<i>Tga1 + Maize/Tga1 + Maize</i>	3964.0	837.260
<i>Tga1 + Maize/tga1 + teosinte</i>	69.3	28.443
<i>tga1 + teosinte/tga1 + teosinte</i>	96.0	42.579

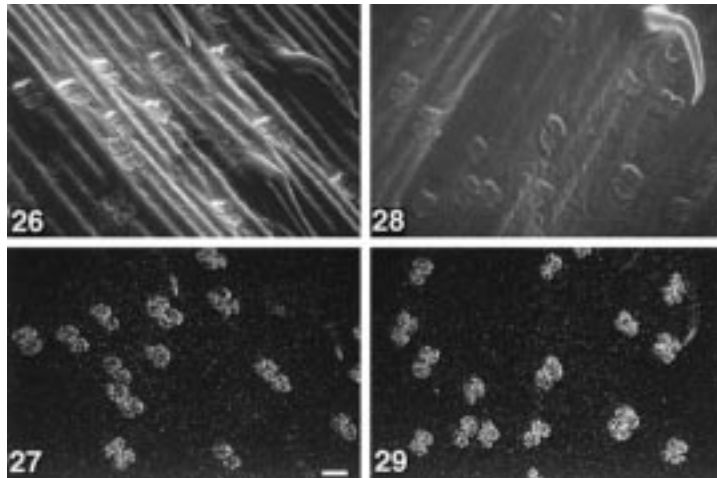
DISCUSSION

We have shown that *teosinte glume architecture1* (*tga1*) has multiple effects on the female inflorescence of maize, and is thus likely to be regulatory in nature. In the W22 background, the effects of the teosinte allele (*tga1+teosinte*) on glume and internode dimensions and glume hardening combine to partially rebuild a teosinte cupulate fruitcase architecture that nearly encapsulates the maize kernels.

First, *tga1+teosinte* enlarges and reshapes several component parts of the cupulate fruitcase, resulting in partial encapsulation of the kernel. It increases the length of each internode, equivalent to the rachid of the cupulate fruitcase, and increases the size of the glume both in thickness and length. Each of these enlargements increases the volume of the fruitcase (cupule) available for the kernel, though not sufficiently to contain the entire kernel. The increased curvature of the glume has a similar effect, though it only succeeds in capturing the base of the kernel, resulting in a constriction of the basal portion of the kernel as it develops. The one structure *tga1+teosinte* shortens is the rachilla. This further enhances the encapsulation of the kernel, as the shorter rachilla helps keep the kernel within the fruitcase cavity.

The timing and position of *tga1* effects suggest that *tga1* expression is restricted to the female inflorescence and begins no later than stage II, when the female pattern of differentiation begins. We have detected no differences among genotypes in the tassel, including no difference in silica deposition. Significant differences for internode length of the female inflorescence among genotypes were apparent by stage II, while differences for glume length and even glume thickness were suggestive, though not significant, this early.

We have shown that *tga1* also has effects at the cellular level. *tga1+teosinte* appears to affect glume thickness by

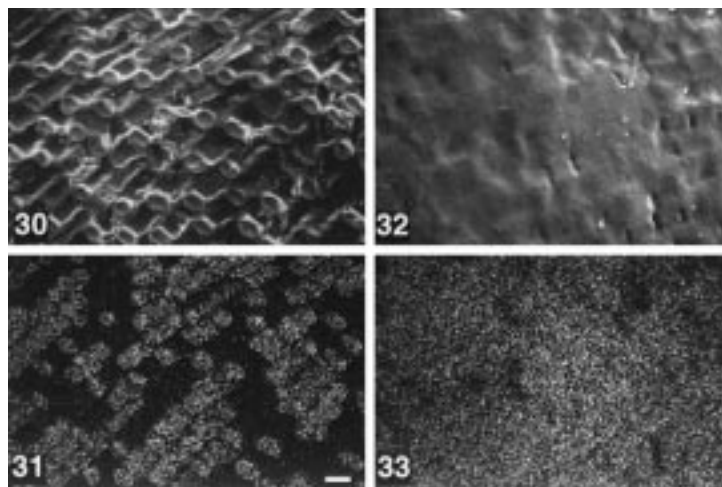


Figs. 26–29. Silica distribution in tassel glumes. SEM micrographs (Figs. 26, 28) of maize tassel glumes and their corresponding silica dot maps (Figs. 27, 29). Genotypes shown are *Tgal+Maize/Tgal+Maize* (Figs. 26, 27), and *tgal+teosinte/tgal+teosinte* (Figs. 28, 29). Bar = 15 μ m for all four images.

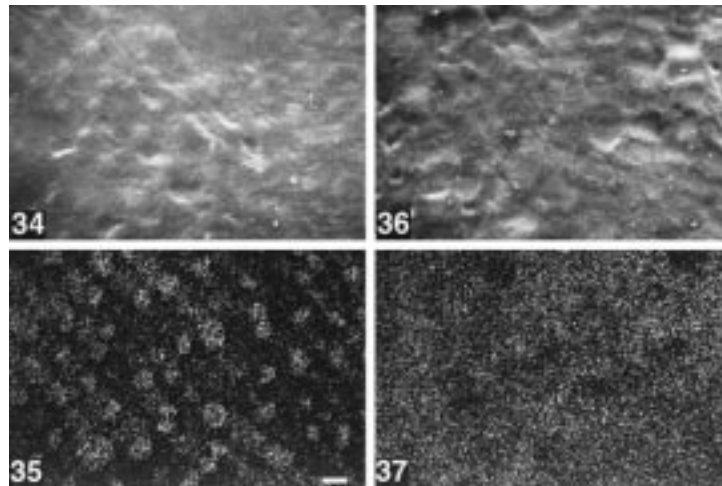
increasing the number of cells comprising the abaxial mesoderm, which becomes lignified. Interestingly, our analyses suggest that those cells in the *tgal+teosinte* homozygote are not as completely lignified as those in the *Tgal+Maize* homozygote. This may be a secondary effect of the thickness. Supportive of this, we have observed that near the side margins of the glume, where the glume is thinner, cells become lignified much earlier than near the center of the glume (J. Dorweiler, unpublished observations). This difference in the degree of lignification may also be a cost–benefit compromise. The cost of increasing the number of cells may be balanced with decreasing energy input toward lignification, with the possible benefit that partial lignification of more cells may actually produce a stronger structure than complete lignification of fewer cells. Our observations confirm that glumes of *tgal+teosinte* homozygotes are actually much more rigid than those of heterozygotes and *Tgal+Maize* homozygotes (Dorweiler et al., 1993).

Our results also suggest that *tgal* regulates which cells of the glume and rachid epidermis become silicified. In the maize background, silica deposition in *Tgal+Maize* homozygotes is limited to specialized silica cells. This pattern is consistent with the silica deposition pattern in the tassel glumes shown here, and that found in most grass leaves (Piperno, 1988). Silica deposition in *tgal+teosinte* homozygotes in the maize background, and either genotype in the teosinte background, can also occur in the epidermal long cells. This reveals that *tgal* is in some way involved in activating the silica deposition pathway in certain cells, or in repressing it in others. The differences due to genetic background suggest that other loci are also involved in this process. The results of silica deposition analyses in teosinte rachids revealed similar effects of *tgal* in determining where silica is deposited. *tgal* also seems to affect the number and distribution of the short silica cells in the epidermis.

The effects of *tgal* on silica deposition have some ar-



Figs. 30–33. Silica distribution in teosinte background. SEM micrographs (Figs. 30, 32) of teosinte glumes and their corresponding silica dot maps (Figs. 31, 33). Genotypes shown are *Tgal+Maize/Tgal+Maize* (Figs. 30, 31), and *tgal+teosinte/tgal+teosinte* (Figs. 32, 33). Bar = 15 μ m



Figs. 34–37. Silica distribution in teosinte rachids. SEM micrographs (Figs. 34, 36) of teosinte rachids and their corresponding silica dot maps (Figs. 35, 37). Genotypes shown are *Tgal+Maize/Tgal+Maize* (Figs. 34, 35), and *tgal+teosinte/tgal+teosinte* (Figs. 36, 37). Bar = 15 μm for

archaeological relevance. Long after most plant material has decomposed, the insoluble silica crystals from within the cells, called phytoliths, remain. Phytolith size and three-dimensional structure can be analyzed to determine the species, and relative proportions, of plants that were growing in a particular area at a given time (Piperno, 1984). There is even some evidence that suggests that maize and teosinte may be distinguishable by the relative proportions of each phytolith type (Piperno, 1984). This difference was determined using leaf tissue. Our results showing the effects of *tgal* and genetic background on cellular deposition of silica in the glume indicate that it will be important to analyze glume phytoliths in an archaeological context.

To our knowledge, *tgal* is the only locus that has been shown to control which cells become silicified. This may prove beneficial for altering the amount of silica incorporated into plants. Of potential importance, silica deposition can affect the dry mass of plants, provide protection from pests, or detrimentally grind down the teeth of herbivores.

Several of the developmental changes conferred by *tgal+teosinte* result in harder, less pliable glumes. *tgal+teosinte* glumes are thicker, composed of more cells which become lignified, and develop a more uniformly silicified epidermal layer. Each of these contributes to the fitness of teosinte, protecting the developing kernel from herbivores such as birds or insects. From a human perspective, these same features complicate the extraction of seeds from the teosinte fruitcase, and are both undesirable and unnecessary under domesticated cultivation. Thus, the important change to *Tgal+Maize* producing more harvestable kernels may have been a critical first step making teosinte a more valuable crop worthy of further domestication.

The major effects of this single locus are strongly supportive of a step-wise evolution of maize from teosinte, rather than a single catastrophic event. Beadle (1972, 1980) argued, and our results support, that maize evolved from teosinte via changes in a small number of genes of large effect. Our results contradict Iltis's (1983) cata-

strophic sexual transmutation theory (CSTT). First, the CSTT explicitly proposed that major genes like *tgal* should not exist. Second, since the CSTT implies that tassel and ear glumes would be of identical origin, they should be of similar structure, and few if any genetic loci should affect one and not the other. The existence of *tgal*, which affects the ear but not the tassel glume, contradicts this expectation. Third, the CSTT fails to consider or explain the fundamental structural differences between tassel and ear glumes. The soft tassel glumes are foliaceous, while the soft glumes of maize female inflorescences are often described as coriaceous or leathery (Galinat, 1970), and could be described as fleshy prior to maturation and dehydration. Thus, maize glumes are more reasonably explained as modified teosinte ear glumes rather than teosinte tassel glumes.

Finally, the major effects of *tgal* support the argument that evolution can proceed via changes of large effect in single genes and is not restricted to proceeding via small changes in multiple genes (Maynard Smith, 1983; Gottlieb, 1984; Orr and Coyne, 1992). Moreover, the major effect of *tgal* may not be due to a loss of function as one sees with numerous recessive mutations, but rather a modification in function or expression. A modification of *tgal* function or expression seems most reasonable to induce an alternative developmental pathway since we see no easy way to reconcile both the semidominance and diverse effects of the maize allele with a simple loss in function. Though evolution is a stochastic process limited to working with the available variation, modification of a regulatory locus seems an expedient manner for effecting major morphological change, and *tgal* represents an excellent example of a single locus having a major evolutionary effect.

LITERATURE CITED

- BACHMANN, K. 1983. Evolutionary genetics and the genetic control of morphogenesis in flowering plants. *Evolutionary Biology* 16: 157–208.
- BEADLE, G. W. 1972. The mystery of maize. *Field Museum of Natural History Bulletin* 43: 2–11.

- . 1980. The ancestry of corn. *Scientific American* 242: 112–119,162.
- CARROLL, S. B. 1994. Developmental regulatory mechanisms in the evolution of insect diversity. *Development* (Supplement): 217–223.
- CHENG, P. C., R. I. GREYSON, AND D. B. WALDEN. 1983. Organ initiation and the development of unisexual flowers in the tassel and ear of *Zea mays*. *American Journal of Botany* 70: 450–462.
- COEN, E. S., AND J. M. NUGENT. 1994. Evolution of flowers and inflorescences. *Development* (Supplement): 107–116.
- CURTIS, D., J. APFELD, AND R. LEHMANN. 1995. *nanos* is an evolutionarily conserved organizer of anterior-posterior polarity. *Development* 121: 1899–1910.
- DOEBLEY, J. 1993. Genetics, development and plant evolution. *Current Opinion in Genetics and Development* 3: 865–872.
- , AND A. STEC. 1991. Genetic analysis of the morphological differences between maize and teosinte. *Genetics* 129: 285–295.
- , AND ———. 1993. Inheritance of the morphological differences between maize and teosinte: comparison of results for two F₂ populations. *Genetics* 134: 559–570.
- DORWEILER, J., A. STEC, J. KERMICLE, AND J. DOEBLEY. 1993. *Teosinte glume architecture 1: A genetic locus controlling a key step in maize evolution*. *Science* 262: 233–235.
- GALINAT, W. C. 1957. The effects of certain genes on the outer pistillate glume of maize. *Botanical Museum Leaflet of Harvard University* 18: 57–76.
- . 1969. The evolution under domestication of the maize ear: string cob maize. *Massachusetts Agricultural Experiment Station Bulletin* 577: 1–19.
- . 1970. The cupule and its role in the origin and evolution of maize. *Massachusetts Agricultural Experiment Station Bulletin* 585: 1–20.
- GOTTLIEB, L. D. 1984. Genetics and morphological evolution in plants. *American Naturalist* 123: 681–709.
- HARRIS, P. J., AND R. D. HARTLEY. 1976. Detection of bound ferulic acid in cell walls of the Gramineae by ultraviolet fluorescence microscopy. *Nature* 259: 508–510.
- HOLLAND, P. W. H., AND J. GARCIA-FERNANDEZ. 1996. *Hox* genes and chordate evolution. *Developmental Biology* 173: 382–395.
- ILTIS, H. H. 1983. From teosinte to maize: the catastrophic sexual transmutation. *Science* 222: 886–894.
- MAYNARD SMITH, J. 1983. The genetics of stasis and punctuation. *Annual Review of Genetics* 17: 11–25.
- ORR, H. A., AND J. A. COYNE. 1992. The genetics of adaptation: a reassessment. *American Naturalist* 140: 725–742.
- PATEL, N. H. 1994. The evolution of arthropod segmentation: insights from comparisons of gene expression patterns. *Development* (Supplement): 201–207.
- PIPERNO, D. R. 1984. A comparison and differentiation of phytoliths from maize and wild grasses: use of morphological criteria. *American Antiquity* 49: 361–383.
- . 1988. Phytolith analysis: an archeological and geological perspective. Academic Press, San Diego, CA.
- RAFF, R. A. 1992. Evolution of developmental decisions and morphogenesis: the view from two camps. *Development* (Supplement): 15–22.
- SYLVESTER, A. W., AND S. E. RUZIN. 1994. Light microscopy I: dissection and microtechnique. In M. Freeling and V. Walbot [eds.], *The maize handbook*, 83–95. Springer-Verlag, New York, NY.
- WILLIAMS, M. H., AND A. W. SYLVESTER. 1994. Scanning electron microscopy. In M. Freeling and V. Walbot [eds.], *The maize handbook*, 108–117. Springer-Verlag, New York, NY.
- ZEYEN, R. J., G. G. AHLSTRAND, AND T. L. W. CARVER. 1993. X-ray microanalysis of frozen-hydrated, freeze-dried, and critical point dried leaf specimens: determination of soluble and insoluble chemical elements at *Erysiphe graminis* epidermal cell papilla sites in barley isolines containing *M1-o* and *ml-o* alleles. *Canadian Journal of Botany* 71: 284–296.